A Mouse Model for Meckel Syndrome Type 3

Susan A. Cook, Gayle B. Collin, Roderick T. Bronson, Jürgen K. Naggert, Dong P. Liu, Ellen C. Akeson, and Muriel T. Davisson

The Jackson Laboratory, Bar Harbor, Maine

ABSTRACT

Meckel-Gruber syndrome type 3 (MKS3; OMIM 607361) is a severe autosomal recessive disorder characterized by bilateral polycystic kidney disease. Other malformations associated with MKS3 include cystic changes in the liver, polydactyly, and brain abnormalities (occipital encephalocele, hydrocephalus, and Dandy Walker–type cerebellar anomalies). The disorder is hypothesized to be caused by defects in primary cilia. In humans, the underlying mutated gene, *TMEM67*, encodes transmembrane protein 67, also called meckelin (OMIM 609884), which is an integral protein of the renal epithelial cell and membrane of the primary cilium. Here, we describe a spontaneous deletion of the mouse ortholog, *Tmem67*, which results in polycystic kidney disease and death by 3 wk after birth. Hydrocephalus also occurs in some mutants. We verified the mutated gene by transgenic rescue and characterized the phenotype with microcomputed tomography, histology, scanning electron microscopy, and immunohistochemistry. This mutant provides a mouse model for MKS3 and adds to the growing set of mammalian models essential for studying the role of the primary cilium in kidney function.

Primary polycystic kidney disease (PKD) is a genetically heterogeneous condition that afflicts as many as 600,000 people in the United States and more than 12 million people worldwide[1,2] (see also http://kidney.niddk.nih.gov/kudiseases/pubs/kustats/index.htm). PKD is inherited as both dominant (ADPKD) and recessive (ARPKD) disorders; the incidence of new cases of ADPKD and ARPKD is one in 1000 and one in 20,000 live births, respectively.[3,4] Renal cystic disease also is a feature of many complex syndromes with other associated abnormalities, such as Von Hippel-Lindau syndrome,[5] Bardet-Biedl syndrome,[6] and Meckel syndrome types 1 through 5[7] (see also http://www.ncbi.nlm.nih.gov/sites/entrez?db=OMIM). The mouse provides an excellent model for elucidating the pathogenesis of human kidney disorders because of the striking anatomic and physiologic similarities of mouse and human kidneys. Mouse models have contributed substantially to understanding the etiology of PKD.[8,9]

We report here a novel mutation, bilateral polycystic kidneys (*bpck*), on mouse chromosome (Chr) 4 that causes juvenile lethality from bilateral PKD. This mutation is a 295-kb deletion that includes the *Tmem67* gene. Orthologs of this gene are mutated in humans with MKS3 and in the *wpk/wpk* (Wistar polycystic kidney) rat.[10] Because the PKD phenotype of *bpck/bpck* mutants mimics the pathology of human MKS3,[7] this first mouse model will be valuable for studying the cause and progression of MKS3 and cystic disease in general, as well as determining the success of diet, drug, and gene therapies.

RESULTS

Phenotype

On a mixed B6C3FeF1/J *a/a* genetic background (see the Concise Methods section), *bpck/bpck* mutants typ-

ically die by 3 wk of age from bilateral polycystic nephropathy (Figure 1, A through C). Some mutants also develop hydrocephalus, usually detectable within a few days of birth (Figure 2). Smaller than their siblings, mutants are visibly obvious by their swollen abdomens resulting from grossly enlarged polycystic kidneys. *bpck/bpck* mutant mice exhibit classic PKD; the number and size of renal cysts increase until only a minimal amount of medulla parenchyma remains (Figure 1B). Enlarged glomeruli are rarely seen. Confocal imaging of kidney sections stained for F-actin shows that the cuboidal epithelium lining the tubules flattens as cysts enlarge (Figure 1D). Preliminary light microscopy with periodic acid-Schiff or hematoxylin and eosin staining ($n = 1$; Figure 1, E through G) shows cysts are detected as early as embryonic day 16 (E16; Figure 1G), the earliest age examined to date. More comprehensive and detailed developmental studies will be required in the future to determine when cysts first appear during embryonic kidney development. Microcomputed tomography shows that the progressive volumetric kidney enlargement is significantly greater in *bpck/bpck* mutants than in controls ($P < 0.0001$; Figure 3). Heterozygotes (+/*bpck*) do not differ from wild-type (+/+) controls; hence, the phenotype is recessive.

Mutant mice die before reaching sexual maturity. Ovaries of *bpck/bpck* females are small but appear normal by light microscopy; however, failure of many transplantations into histocompatible or immune-deficient hosts suggests ovarian dysfunction. Mutant testes are much smaller than those of control littermates (Figure 1A). At 3 wk of age, the progression of maturing cells from spermatocytes to spermatids in mutant testes seems disorganized with degenerating cells present (data not shown). All other tissues appear normal by light microscopy. Mutants do not show hepatic ductal dysplasia and cysts, polydactyly, occipital encephalocele, or cerebellar defects, features present in some patients with MKS3. Light microscopy of brains stained with hematoxylin & eosin from seven postnatal day 14 (P14) and nine P20 mutants showed no cerebellar abnormalities and the same number of cerebellar folia as in littermate controls. Although some mice showed the retinal degeneration common to C3H strains, the retinas of mutants have not yet been studied in detail.

Elevated blood urea nitrogen at 2 wk of age can predict mutants before they near ESRD but not early enough to study development. *bpck* homozygotes seem anemic by crude hematocrit measurements (data not shown). Plasma urea nitrogen values of azotemic mutants are significantly higher than in controls, ranging from 57 to 105 mg/dl (mean ± SEM 73.06 ± 13.19; $n = 18$).
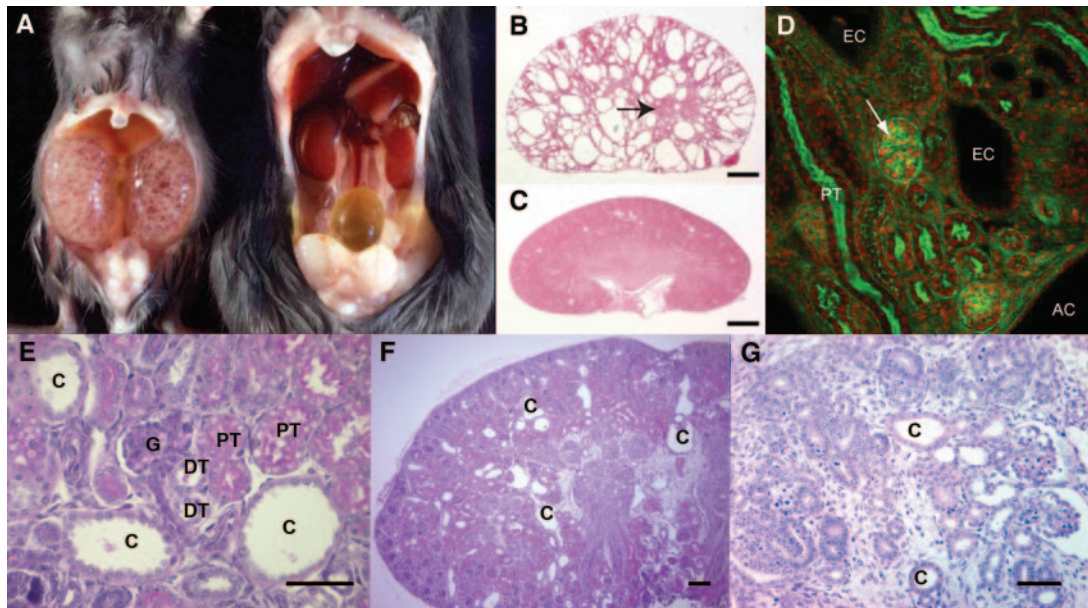

Figure 1. Gross appearance and histopathology of *bpck/bpck* and control kidneys. (A) Autopsy image of an 20-d-old *bpck/bpck* male with ESRD (left) and normal (genotype undetermined) male sibling control (right). Mutant kidneys are bilaterally polycystic and grossly enlarged. Mutant testes are much smaller than those of the control. Viscera in both mutant and control were excised for visibility. (B) *bpck/bpck* kidney from A. The cortex and medulla have been destroyed by cysts; only a small section of medulla parenchyma remains (arrow). (C) Normal kidney from sibling control with cortex and medulla intact. Bars = 1 mm. Both are hematoxylin & eosin stained. (D) Confocal image of *bpck/bpck* renal cortex at 17 d. Some residual glomeruli (arrow) and tubules remain in the interstitium. Two early cysts (EC) with cuboidal epithelium and an advanced cyst (AC) with flattened cuboidal epithelium are visible. Stains are phalloidin (green) for F-actin, located in brush border membranes and cellular cytoplasm, and topro3 (orange) for nuclei. The proximal convoluted tubule (PT) in longitudinal section has tall epithelium with a brush border staining strongly for actin, whereas cyst epithelium has very little cytoplasmic actin. The epithelium in cystic tubules resembles that of distal convoluted tubules rather than that of proximal tubules. (E through G) Histopathology of cystic tubules in *bpck/bpck* mutants at P0 (E and F) and E16 (G; all periodic acid-Schiff stained; bars = 50 µm). Normal tissues are glomerulus (G), distal tubule (DT), and proximal tubule (PT). Some cystic tubules (C) are evident.
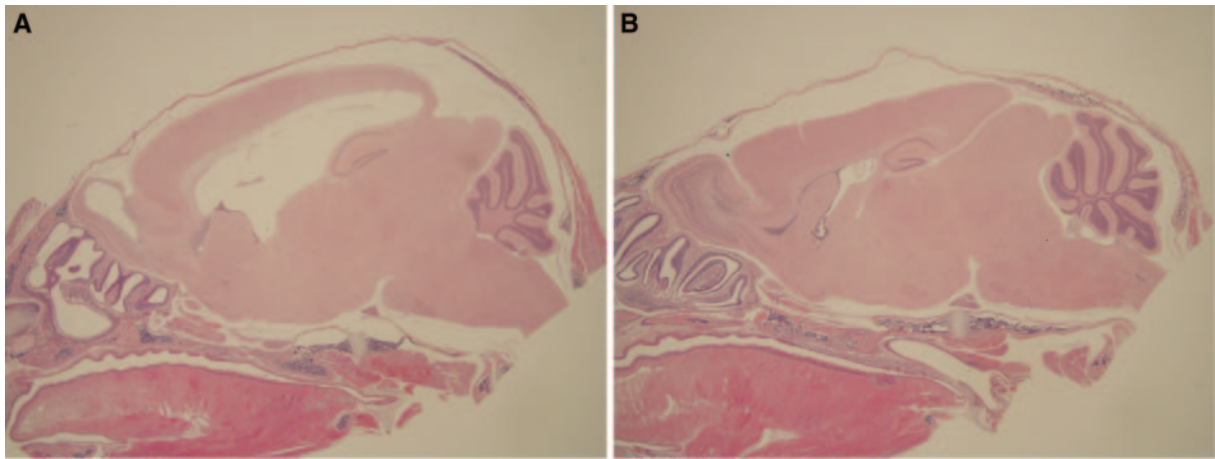
Figure 2. (A and B) Hydrocephalus in a 2-wk-old *bpck/bpck* mutant (A) compared with a normal littermate control (B). Hematoxylin and eosin stain.
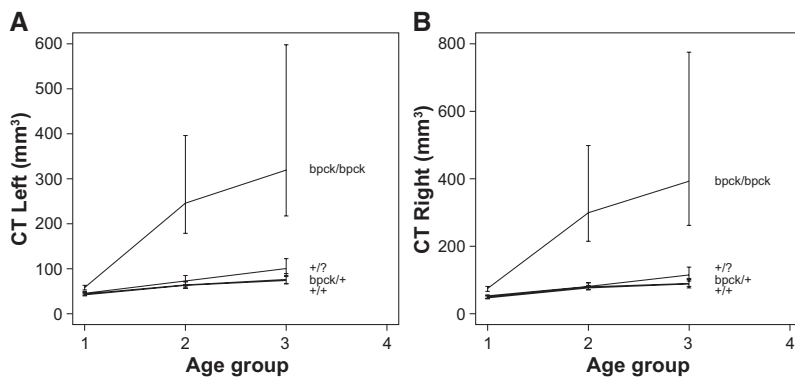

Figure 3. Plots showing progressive enlargement of kidneys in mutants compared with controls (+/+, +/*bpck*, and +/?). (A) Left kidney. (B) Right kidney. Ages of mice in group 1 are 9 to 12 d (*n* = 6 mutants, 19 controls), in group 2 are 15 to 17 d (*n* = 6 mutants, 15 controls), and in group 3 are 19 to 22 d (*n* = 6 mutants, 13 controls). The original computed tomography volume data were skewed to the right, and inverse transformation was applied to stabilize the variance. Linear mixed model with repeated measure analyses were performed[42] with SAS 9.1.3 (SAS Institute, Cary, NC).

Wild-type and heterozygotes ranged from 17 to 30 mg/dl (mean ± SEM 23.30 ± 4.79; *n* = 10).

Scanning electron micrographs of *bpck/bpck* mutant kidneys show mild dilation of some proximal tubules and severe enlargement of renal distal collecting tubules as identified by the presence of intercalating or identifying cells (Figure 4). At birth (P0), the primary cilia on the epithelial cells in these cystic tubules appear dysmorphic and vary in length. By P3, some cilia are elongated, and by P14, many are elongated (Figure 4). Cilium measurements in the distal nephron segments at P14 and P20 (Table 1) show that mutant cilia are significantly longer than +/*bpck* or +/+ controls. Our analysis confirmed the observation by others[11] that cilia were shorter in older (P34, 15 wk) adult wild-type mice than in young wild-type mice. Proximal tubules containing brush border were infrequently dilated in mutants; thus, few cilia were measured in these regions. However, the few cilia we were able to measure in the mutants' proximal tubules and parietal epithelium of Bow-

man's capsule were elongated (Figure 4); this needs further investigation. Although several primary cilium defects have been associated with *situs inversus*, we have not seen laterality anomalies in *bpck/bpck* mutants.

Immunohistochemistry using antibodies that distinguish proximal tubules, connecting tubules, distal convoluted tubules, and collecting ducts (see the Concise Methods section) suggests that early postnatal cysts form predominantly in distal segments of the renal tubules. In P3 to P5 mutants, the majority of cysts are in cortical distal tubules with some cysts in collecting ducts. At P14, the majority of cysts are in collecting ducts and collecting tubules. At both ages P5 and P14, proximal tubules seem normal or only slightly dilated (Figure 5).

Genetic Mapping
By analysis of 2120 meioses in an intercross with CAST/EiJ, we mapped the *bpck* mutation to an approximately 0.6-cM interval on Chr 4 between *D4Mit261* (11.55 Mb) and *D4Mit19* (12.11 Mb). All Chr 4 physical locations are taken from Ensembl release 48, NCBI build m37. PCR analysis of the *Cdh17* (cadherin 17) gene found a deletion from bp 11,724,161 in intron 10 (ENSMUSG00000028217) through the last exon (exon 18). Further PCR showed that the deletion extends to bp 12,019,908 in intron 2 of *C430048L16Rik* (ENSMUS00000052317). This deletion of 295 kb affects six candidate genes: *Cdh17*, *Ppm2c* (protein phosphatase 2C, magnesium dependent, catalytic subunit, ENSMUSG00000049225), a gene predicted from adult testis cDNA (ENSMUSG00000073995), *1700123M08Rik* (Riken cDNA 1700123M08 gene, OTT-MUSG00000004564), *Tmem67* (ENSMUSG00000049488), and *C430048L16Rik* (RIKEN cDNA C430048L16 gene; Figure 6). The deletion is not cytologically detectable by G-band analysis. Proximal flanking markers *D4Mit264* (9.32
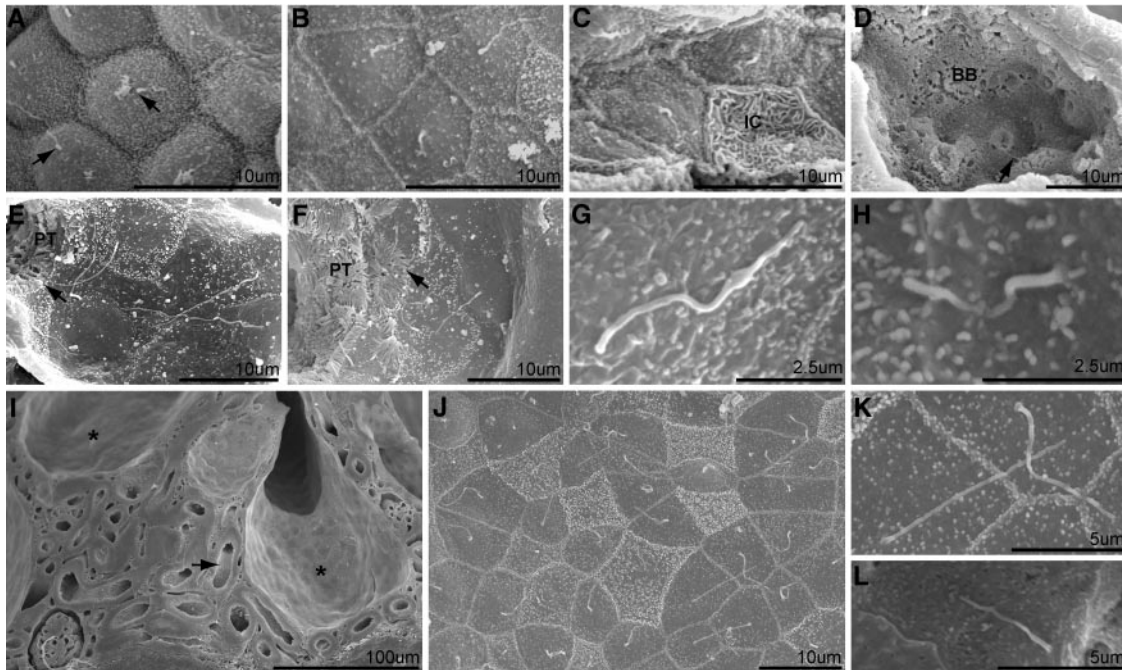
Figure 4. Ultrastructural analysis of cilia in *bpck/bpck* cystic kidneys. (A) A renal cyst of collecting duct origin from a *bpck/bpck* mutant taken soon after birth. Each principle cell contains a cilium along with unidentified debris. Arrows demarcate the base of the cilia. (B and C) Distal connecting tubules in a P3 b*pck/bpck* mutant (B) and control (C). IC, intercalated cell. (D) Low-magnification view of an enlarged P3 *bpck/bpck* proximal tubule (PT) with an elongated primary cilium (arrow) extending above the brush border (BB). (E) Elongated cilia are observed in the parietal epithelium of the Bowman's capsule in a 2-wk-old *bpck/bpck* mutant. (F) Age-matched control cilia. The arrows depict the urinary pole where glomerular infiltrates drain into the proximal tubule. (G and H) High-magnification view of a P14 *bpck/bpck* elongated cilium (G) and an age-matched control cilium (H) from a distal connecting segment of the nephron. (I) A 3-wk-old *bpck/bpck* kidney at low magnification. *Non-BB renal cysts; arrow demarcates a proximal tubule. A normal-appearing glomerulus is seen in the bottom left corner. (J) Surface of a non-BB cyst in a distal tubule from a 3-wk-old *bpck/bpck* mouse. Different lengths of cilia are visible. (K and L) High-magnification view of cilia is shown in a *bpck/bpck* mutant (K) and a wild-type control (L). Specimens were mounted and examined by a Hitachi S3000N scanning electron microscope at 20 kV. Magnifications: ×4500 in A through C; ×3000 in D through F; ×7000 in G, H, K, and L; ×450 in I; ×2300 in J.

Mb), *D4Mit101* (9.62 Mb), and single-nucleotide polymorphism rs27732337 (11.52 Mb) and distal flanking markers *D4Mit135* (19.78 Mb) and *D4Mit268* (20.54 Mb) show that the region spanning the *bpck* mutation is derived from its ancestral B6 chromosome.

Delimiting the deletion enables quantitative PCR (qPCR) assays to identify wild-type, heterozygous, and mutant *bpck* mice (Figure 7A). *Apob* (apolipoprotein B) on Chr 12 was used as the endogenous control. Primer and probe sequences are listed in Table 2 (1 through 9). The deletion shows stable inheritance as genotypes at both ends (*Cdh17* and *C430048L16Rik*) have always agreed. Genotyping facilitates *bpck* colony maintenance and allows molecular and histopathologic studies at ages before the mutant phenotype becomes visibly obvious.

To confirm that the deletion is devoid of any extraneous insertion, we designed primers in intron 10 of *Cdh17* (Table 2, 10) and in intron 2 of *C430048L16Rik* (Table 2, 11) to span the deleted region. We amplified a product in *bpck/bpck* mice but not wild-type controls. Sequence analysis showed a contiguous 1312-bp segment with BLAST results verifying with 99% identity that bp 1 through 1041 match wild-type *C430048L16Rik* and bp 1042 through 1284 match *Cdh17*.

Identification of *TMEM67* as the gene mutated in humans with MKS3[10] implicated *Tmem67* as the gene responsible for the mouse *bpck* mutation. On the basis of the temporal and spatial expression of *Tmem67* in the SymAtlas database (http://wombat-.gnf.org/SymAtlas/), we used reverse transcription–PCR and primers within exons 12 and 13 of ENSMUST00000050686 (Table 2, 12 and 13) to confirm that *Tmem67* cDNA is amplified in kidney, liver, and brain of P8 +/*bpck* and +/+ mice. This 100-bp product is absent from these tissues in *bpck/bpck* mutant siblings (Figure 7B).

For direct evidence that the deletion of *Tmem67* causes PKD in *bpck/bpck* mice, we used transgenic rescue with four overlapping bacterial artificial chromosomes (BACs; Figure 6). From crosses with mice of three transgenic lines carrying BAC RP23-203A12 and four lines carrying BAC RP24-229O13 (both BACs contain the *Tmem67* gene), *bpck/bpck* mice with either of the two transgenes are alive beyond 1 yr of age with no symptoms of PKD or hydrocephalus. Sibling

Table 1. Cilium measurements on SEM preparations of distal tubules, collecting ducts, and tubules[a]

Genotype	No. of Cilia (No. of Mice)	Cilia Length (μm; Mean ± SD)
B6C3FeF1-*bpck* colony (no Tg)		
bpck/bpck		
P14/15	54 (3)	6.40 ± 1.40
3 wk	57 (5)	6.30 ± 1.30
+/*bpck*		
P14/15	30 (3)	4.60 ± 0.80
3 wk	21 (3)	3.30 ± 0.90
+/+		
P14/15	32 (3)	4.90 ± 1.30
3 wk	17 (2)	4.03 ± 0.68
Transgenic rescue crosses		
bpck/bpck no Tg		
P34	12 (1)	5.40 ± 1.53
7 to 8 wk	46 (4)	6.20 ± 2.00
bpck/bpck Tg		
P34	30 (3)	2.80 ± 0.45
7 to 8 wk	63 (6)	2.70 ± 0.43
+/*bpck* no Tg		
P34	10 (1)	2.90 ± 0.57
+/*bpck* Tg		
P34	20 (2)	2.80 ± 0.49

[a]B6C3FeF1-*bpck* colony:
bpck/bpck versus +/*bpck* and +/+ controls at P14/P15: $P = 0.0367$.
bpck/bpck versus +/*bpck* and +/+ controls at 3 wk: $P = 0.0015$.
Transgenic rescue crosses versus B6C3FeF1-*bpck* colony:
bpck/bpck P14/15 versus *bpck/bpck* Tg 7 to 8 wk: $P = 0.0007$.
bpck/bpck 3 wk versus *bpck/bpck* Tg 7 to 8 wk: $P < 0.0001$.
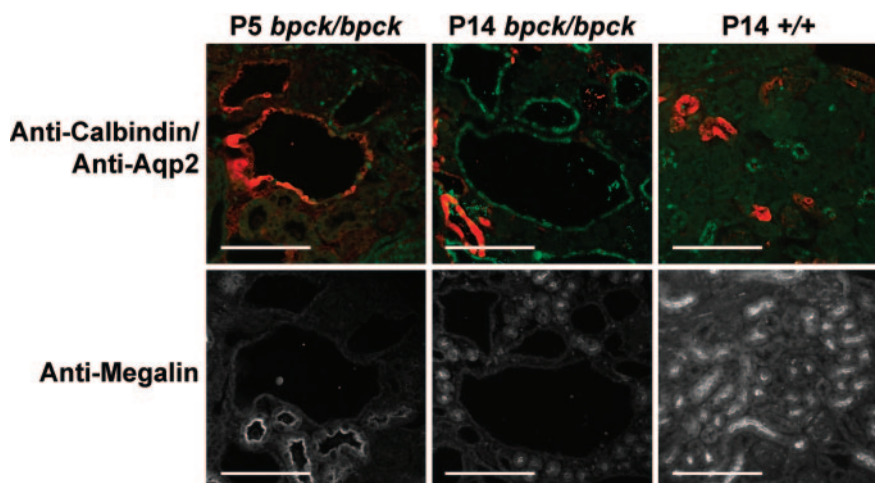Transgenic rescue crosses:
bpck/bpck no Tg versus Tg at P34: $P < 0.0001$.
bpck/bpck no Tg versus Tg at 7 to 8 wk: $P = 0.0288$.
bpck/bpck with Tg at P34 versus all +/*bpck* (with Tg and no Tg) at P34: $P = 0.9151$.

mutants without the transgenes developed PKD, and most died at 17 to 20 d (Table 3). No *bpck/bpck* mutants without a transgene survived beyond 8 wk. Histopathology showed that the *Tmem67*-containing transgenes rescued the PKD phenotype as well (Figure 8). All seven transgenic lines involving these two BACs gave equivalent success.

Figure 5. Immunohistochemical characterization of cystic tubules in *bpck/bpck* mutant kidneys. (Top) P5 and P14 renal tubules double stained with anti-calbindin (red) and anti–aquaporin 2 (Aqp2; green). (Bottom) Adjacent sections of P5 and P14 renal tubules stained with anti-megalin (white). In the younger mutants (P5), the cysts are found primarily in cortical distal tubules (red), with some in collecting ducts (green) and connecting tubules (red/green); some proximal tubules (white) show mild dilation. In the older mutants (P14), the majority of cysts are in the collecting ducts (green). Immunostained sections from a P14 wild-type control are shown on the far right. Bar = 100 μm.

The genetic classes of progeny from the *Tmem67* transgenic rescue crosses show the Mendelian results expected for an intercross with the *bpck* recessive mutation and a backcross with the transgene. Of the 126 mice typed for the transgene, 66 (52.4%) carried the transgene. Of the 164 mice typed for *bpck* (those with and without the transgene), there were 40 (24.4%) *bpck/bpck*, 81 (49.4%) +/*bpck* and 43 (26.2%) +/+. More than twice as many *bpck/bpck* transgenic mice ($n = 29$) as *bpck/bpck* nontransgenic mice ($n = 11$) were produced, suggesting that the transgene rescued mutants that would have died pre- or perinatally. A deficiency of mutants also is seen in the maintenance colony (with no transgene; 20.5% mutants from heterozygous parents).

Measurements of distal and collecting tubule cilia in P34, 7- to 8-wk-old, 15-wk-old (Table 1, Figure 9), and 1-yr-old (not shown) *bpck/bpck* transgenic mice show that the elongated cilium phenotype also was rescued. Cilia length in *bpck/bpck* transgenic mice was the same as those from heterozygous or wild-type siblings with or without a transgene. Cilia in 5- to 8-wk-old *bpck/bpck* transgenic mice were significantly shorter than those in the few surviving littermate mutants with no transgene and those in the 3-wk-old *bpck/bpck* mutants from the maintenance colony. Genetic background seems to modulate the effect of TMEM67 on cilium length, because in all genotypes from rescue crosses (transgenes are on C57BL/6J), cilia were generally shorter than those seen in the same genotypes of the B6C3Fe-*bpck* maintenance colony.

The other five genes in the deleted segment were ruled out because (*1*) the two BAC transgenes containing *Tmem67* were the only ones to rescue the phenotype and (*2*) other genes present in these BACs also were present in BACs that failed to rescue (BACs RP23-59K6, two transgenic lines carrying *Cdh17*, and RP23-31I19, four transgenic lines carrying *Ppm2c* and the two predicted genes ENSMUSG00000073995 and *1700123M08Rik*; Figure 6). *C430048L16Rik* was not present in any of the BACs, including the ones that rescued; therefore, none of the other genes in the interval rescues the phenotype, whereas only *Tmem67* does. This argues against a contiguous gene syndrome.

P5 bpck/bpck   **P14 bpck/bpck**   **P14 +/+**

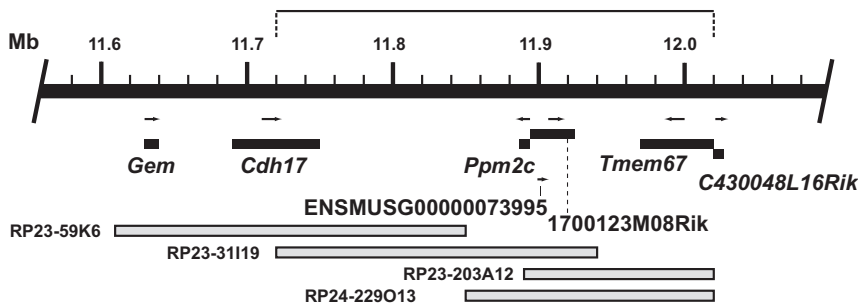**Anti-Calbindin/ Anti-Aqp2**

Anti-Megalin

Chr 4

Figure 6. Diagram of the *bpck* deletion showing the six genes identified within the deleted region and the BACs used for transgenic rescue experiments. BACs RP23-59K6 and RP23-31I19 failed to normalize the mutant phenotype. BACs RP23-203A12 and RP24-229O13 (which contain *Tmem67*) successfully rescued. The gene *C430048L16Rik* was not present in either BAC that rescued. For simplicity, not all predicted genes are included in the diagram. Arrows indicate direction of transcription.

DISCUSSION

Proteins involved in transmembrane ion transport and signal transduction, cell proliferation and differentiation, loss of planar polarity of tubular epithelial cells, and ciliary function have been implicated in PKD.[9] One of the most popular and evolving pursuits in PKD research is the role of primary cilia.[12,13] Cilia occur on a great variety of vertebrate cells[14] and affect internal laterality patterning, signal transduction, and cystic disease. The role of primary cilia in PKD has been explored by analysis of mutations in several cilium-associated genes involved in human disorders and mouse models.[15,16] Currently, the hypothesis is that the primary cilium plays a mechanosensory role by sensing the flow of fluid in renal tubules and activating intracellular signaling pathways. Polycystin 1 and polycystin 2, encoded by *PKD1* and *PKD2*, respectively, are transmembrane proteins in the ciliary membrane that putatively mediate this mechanosensory function.[17,18] Deflection of the primary cilium by fluid flow activates a signaling pathway that regulates epithelial cell growth and proliferation by modulating changes in intracellular calcium ions.[17,19] Loss of either polycystin 1 or 2 in humans causes PKD *via* clonal expansion of renal epithelial cells leading to cystic ducts.[18,20] Mice with targeted mutations in *Pkd1* and *Pkd2* show that both genes are essential for normal kidney development and function.[21,22] The gene mutated in human ARPKD (polycystic kidney and hepatic disease 1 [*PKHD1*])[23,24] also has been implicated in cell proliferation and cellular adhesion/repulsion.[25] This protein also has transmembrane domains and is expressed in fetal and adult kidney tissue.

Primary cilia grow by antegrade intraflagellar transport (IFT) of proteins synthesized in the cytoplasm. The proteins
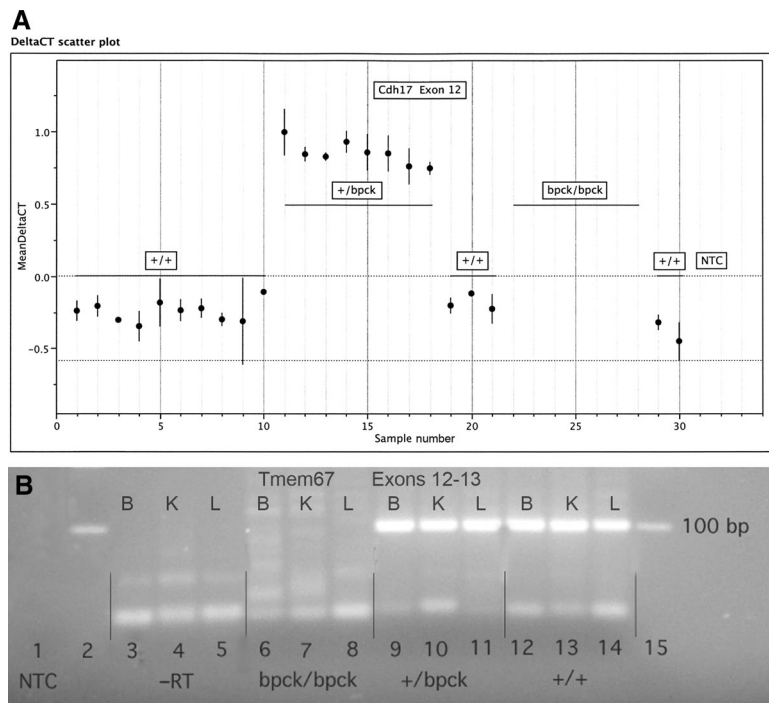

Figure 7. (A) Scatterplot from qPCR showing genotyping of all three genotypes (+/+, +/*bpck*, and *bpck*/*bpck*) from *bpck* colony mice using genomic DNA from tail tips. The genotypes are determined using probes for both ends of the deletion, *Cdh17* being at the 5′ end. qPCR for *Tmem67* gives identical results. Samples 22 through 28 show that no ΔCT calculation from *bpck*/*bpck* mice was possible because there was no fluorescence response to the *Cdh17* probe, which is within the deletion; however, these mutants did show appropriate fluorescence response to the endogenous control probe *Apob*. qPCR reactions were run and analyzed on a 7500 Real Time PCR System (http://www.appliedbiosystems.com). Scatterplots were made with JMP 6.0 (http://www.jmp.com) from SAS Institute. Samples 31 and 32 are no template control (NTC). (B) Expression analysis of *Tmem67* by PCR with cDNA templates: B, brain; K, kidney; L, liver. Lane 1, NTC; lanes 2 and 15, 100-bp ladder; lanes 3 through 5, RT reaction mix minus reverse transcriptase to detect genomic DNA contamination; B, brain of *bpck*/*bpck*; K, kidney of +/*bpck*; L, liver of +/+; lanes 6 through 8, cDNA amplification with *bpck*/*bpck* tissues; lanes 9 through 11, cDNA amplification with +/*bpck* tissues, lanes 12 through 14, cDNA amplification with +/+ tissues. All samples except NTC are from P8 siblings and contain 300 ng of template per 40 μl of reaction. The lack of the 100-bp product from the *bpck*/*bpck* samples using primers from exons 12 and 13 (Table 2, 12 and 13) is representative of many cDNA PCR reactions done with exonic primers throughout the *Tmem67* sequence and results from multiple mice.

Table 2. Primers and TaqMan probes for PCR analysis

ID	Orientation	Sequence (5′→3′)	bp Location (5′→3′)[c]	Gene
1	F	TGGAAGCAAGACTCTGTCTGAAGA[a]	11,726,710-733	*Cdh17*, exon 12
2	F (probe)	6FAM–ACCGCCATCGGATCCACCATCC–TAMRA[a]	11,726,735-756	*Cdh17*, exon 12
3	R	TCAGCATCTGTAGCTTGGATGATT[a]	11,726,781-758	*Cdh17*, exon 12
4	F	TGCCCTGTTTTTCTCAGGTTTAA[a]	12,016,180-202	C430048L16Rik, 5′
5	R (probe)	6FAM–TGCAGAGTTTTCCATCCTCTCCTGTGATTTCT–TAMRA[a]	12,016,235-204	C430048L16Rik, 5′
6	R	GAACCGCTTTGGAAGTGGAA[a]	12,016,258-239	C430048L16Rik, 5′
7	F	CACGTGGGCTCCAGCATT[a]	8,017,294-311	*Apob*, exon 25
8	F (probe)	VIC–CCAATGGTCGGGCACTGCTCAA–TAMRA[a]	8,017,319-340	*Apob*, exon 25
9	R	TCACCAGTCATTTCTGCCTTTG[a]	8,017,367-346	*Apob*, exon 25
10	F	CCCTTTTGTCAAGAAAGATG[b]	11,724,142-161	*Cdh17*, intron 10
11	R	GCAGTCTGCCTCTCACTAAC[b]	12,019,927-908	C430048L16Rik, intron 2
12	F	GAAGAGCAGCACCGTTACCT[b]	11,990,899-918	*Tmem67*, exon 12
13	R	GCCACTTGCTGGAGCTACTGT[b]	11,990,203-182	*Tmem67*, exon 13

[a]Primers and TaqMan probes were designed with PrimerExpress 2.0 (Applied Biosystems). All TaqMan probes were also purchased from AB (http://www.appliedbiosystems.com).
[b]Primers were designed with Primer3 (primer3_www.cgi 0.2). These and primers[a] were purchased from IDT (http://www.idtdna.com).
[c]All genomic locations are from Ensembl release 40 NCBI build m37.

Table 3. Number of mice in each genetic class from transgenic rescue crosses for all progeny typed for both the *bpck* mutation and the transgene[a]

	Genotypes Affected	Genotypes Unaffected				
	bpck/bpck	*bpck/bpck*	+/*bpck*		+/+	
Transgenic Line Used in Cross	No Tg	Tg	No Tg	Tg	No Tg	Tg
203A12, one single copy Tg line	2	5	9	11	2	3
203A12, one multicopy Tg line	1	3	4	4	1	1
229O13, five multicopy Tg lines	8	21	9	11	6	6
Total for all lines	11	29	22	26	9	10

[a]Affected mice developed PKD; unaffected mice still survive beyond 1 yr of age. No mutants without a transgene survived beyond 8 wk of age.
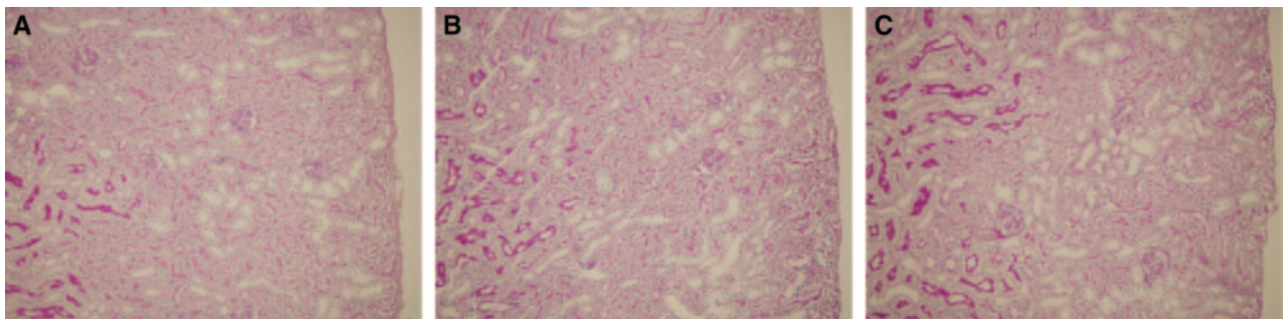
Figure 8. Histopathologic illustration of transgenic rescue in 15-wk-old mice by a BAC containing the *Tmem67* gene. (A) *bpck/bpck* with transgene showing complete rescue of cystic disease. (B) +/+ littermate control with transgene showing no apparent effect of the transgene on tubules. (C) +/+ littermate control without the transgene. Periodic acid-Schiff stain; Bar = 10 μm.

are transported along the ciliary axoneme (microfibrillar structure) from the base of the cilium to the cilium tip where they are assembled into the cilium components.[26] When the cilium reaches "normal" length, elongation ceases and the cilium is maintained by antegrade IFT balanced by retrograde transport of proteins from the cilium tip back to its base. The mechanism of regulation of cilium length is unknown, but proteins involved in IFT (structural proteins in IFT particles and proteins required for loading, unloading, or transporting IFT particles) and in cellular proliferation have been implicated. In the mouse, the polaris protein, encoded by the intraflagellar transport 88 homolog gene (*Ift88*), and the IFT kinesin protein, encoded by the *Kif3a* gene, are required for cilium assembly and normal cilium length. Homo-
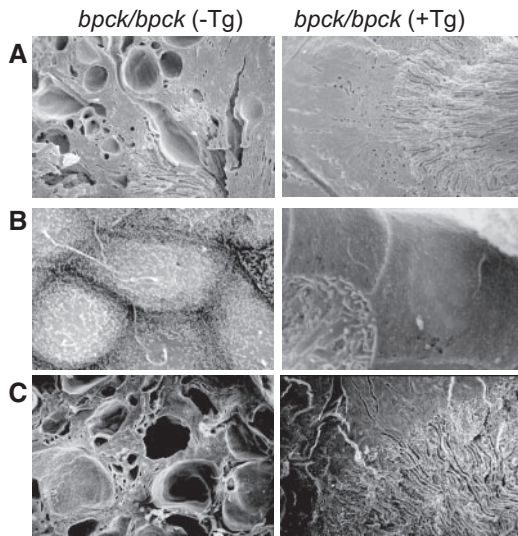
bpck/bpck (−Tg)   bpck/bpck (+Tg)

Figure 9. (A through C) Ultrastructural views of *bpck/bpck* kidneys without (−Tg) and with (+Tg) transgene showing transgenic rescue of P34 (A), P34 (B), and 7-wk *bpck/bpck* (C) −Tg and 15-wk *bpck/bpck* +Tg kidneys, respectively. Magnifications: ×100 in A and C; ×7000 in B.

zygosity for null mutations of either gene in mice causes embryonic lethality.[27,28] Mice with the Oak Ridge polycystic kidney (*Ift88^Tg737Rpw*) hypomorphic mutation in the polaris gene have shortened cilia[28,29]; overexpression of polaris in transgene-rescued *orpk* mutants causes elongated cilia.[11] Polaris is a component of IFT particles and localizes to the basal body and the axoneme of cilia.[30] Polaris and the cystin 1 protein, encoded by *Cys1*, co-localize in renal cilia with polycystin 1 and 2.[31] The *jck* (juvenile cystic kidney) mutation in the *Nek8* gene, encoding NIMA (never-in-mitosis A) protein kinase, causes elongated cilia accompanied by a relocalization of NEK8 from the apical surface to the cytoplasm as well as enhanced accumulation of polycystins 1 and 2 in the ciliary membrane, suggesting NEK8 also plays a role in controlling cilia length.[32] A targeted mutation in the mouse ortholog of one of the human Bardet-Biedl syndrome genes (*Bbs4*), which encodes a protein that localizes to the basal body, also causes PKD and elongation of the primary cilia in renal tubules.[33]

Meckelin (TMEM67), the protein affected in patients with MKS3, also is a ciliary protein associated with PKD and ciliogenesis. It is a transmembrane protein ubiquitously expressed in human embryos with high levels of expression in the kidney, midbrain, liver, and digits.[10,34] The clinical phenotypes of Meckel syndrome and cilium-associated kidney diseases have documented similarities.[10,34] Abnormal cilia also are involved in some forms of hydrocephalus,[35] which is sometimes present in *bpck/bpck* mutants, patients with MKS3, and the *wpk/wpk* mutant rat.

In cultured renal tubule epithelial cells, TMEM67 is localized in the cellular and cilium membranes.[34] Silencing of the *TMEM67* (MKS3) transcript in renal cell cultures caused a marked reduction in cilium formation; thus, TMEM67 is essential for cilium growth either directly or through its interaction with MKS1, a protein that is expressed in the basal body and centrosome.[34] In contrast, the *bpck* null mutation causes cilium elongation, clearly demonstrated by our cilium measurements in multiple mutants and controls at P14 and P20. It is not obvious why reducing the level of TMEM67 protein by siRNA knockdown would reduce the number of cilia,[34] whereas total absence would cause elongated cilia. Possibly in the absence of TMEM67 other proteins replace its role in interacting with MKS1 protein in the centriole's migration to the apical membrane (hypothesized to be required for ciliogenesis on the basis of the siRNA experiments). Reduced levels may be sufficient for this interaction but insufficient to enable centriole migration. Alternatively, the absence of TMEM67 in the cilium membrane could result in no biofeedback to regulate the cilium growth. Finally, the difference could be the differences between *in vivo* and in *vitro* systems. Our data are consistent with the targeted knockout of the Bardet-Biedl syndrome 4 homolog (*Bbs4*) gene in mice. Cilia in primary renal cultures from these mice are shorter after 7 d in culture but significantly longer than controls after 10 d in culture. Also, cilia are longer in 3- to 4-mo-old *Bbs4* mutant mice than in controls. Perhaps TMEM67-siRNA–transfected cultures would produce elongated cilia if allowed to propagate longer in culture than 96 h. To determine whether absence of TMEM67 in *bpck/bpck* mutants affects the basal bodies from which cilia originate will require transmission electron microscopic analysis.

In the rescue crosses, a few *bpck/bpck* mice lacking the transgene survived to 8 wk of age. Such survival is infrequently observed in the maintenance strain as well. Because the rescue crosses and maintenance strain have mixed genetic backgrounds, the variability in PKD onset suggests one or more segregating modifier genes that modulate the severity of the disease. Failed attempts to make either C57BL/6J (B6) and C3H/HeJ (C3) congenic strains (few surviving *bpck/bpck* pups were identified in the litters genotyped) suggests that alleles conferring increased severity and embryonic lethality come from both the B6 and C3 backgrounds.

Although five other genes are affected by the *bpck* deletion, all of the phenotypic defects we have characterized can be attributed to deletion of the *Tmem67* gene on the basis of comparison with MKS3. *Tmem67* is further implicated as the gene responsible for the *bpck* phenotype by the complete rescue from PKD, abnormal cilia, and hydrocephalus by multiple lines of two different BAC transgenes containing the *Tmem67* gene. We cannot rule out that one of the other five genes in the deletion has a minor effect on the phenotype. *Cdh17* encodes a nonclassical cadherin expressed on B lymphocytes; the targeted mutation has not been reported to cause any of the phenotypes observed in *bpck/bpck* mice.[36] We have not studied B cells in *bpck/bpck* mice. The *Ppm2c* gene functions in the mitochondrial pyruvate dehydrogenase multienzyme complex. Deficiencies in humans have not been associated with specific

phenotypes.[37] *C430048L16Rik* could contribute to the phenotype by regulating gene expression because it contains an RNA-binding motif. RNA-binding proteins modulate gene expression by regulating both coding and noncoding RNAs.[38] The gene ENSMUSG00000073995 predicted from adult mouse testis cDNA is not yet characterized for expression in other tissues, and the *1700123M08Rik* gene seems to be noncoding. Transgenic BACs containing any of these genes but lacking *Tmem67* failed to rescue any of the *bpck* phenotype.

Although neither the *wpk/wpk* rat nor the *bpck/bpck* mouse precisely mimics all of the clinical anomalies of MKS3, they provide valuable models for studying the primary pathology, PKD, which is present in 100% of patients. Phenotypic variation can likely be attributed to genetic background modulation, species differences, and/or the result of different mutation types or sites within the gene. Mutations in human MKS3 include two frameshift deletions in exons 3 and 6, two splicing mutations at exons 9 and 15, and a nonconservative missense substitution in exon 11.[10] The bp change in exon 12 of the rat *wpk* gene causes a nonconservative proline-to-leucine substitution at amino acid 394.[10] The mouse *bpck* mutation deletes the entire gene. Because the phenotypes in the *bpck/bpck* mouse and the *wpk/wpk* rat[39,40] are nearly identical, the *wpk* mutation also may cause a null allele.

Although these studies support the causative effect of cilium changes in PKD, cilium length also can respond to environmental changes initiated by renal injury. Tubule enlargement resulting from mechanical ureteral obstruction in C57BL/6 mice caused cilium elongation, and reversal of obstruction returned the cilia to normal length.[41] These results support the mechanosensory role of primary cilia and implicate them in the injury/repair process. Finally, cilium changes are only part of the mechanism of PKD, because, at least in the case of polaris, differences in cilium length have been genetically dissociated from cystic disease. *orpk* mutants with short cilia, *orpk* transgenic mice with elongated cilia, and polaris knockout transgenic rescue mice with normal length cilia all develop cystic disease, albeit late onset in the two rescue mice.[11]

The localization of the TMEM67 protein to the ciliary membrane in normal human tissues; the phenotypic similarities of our mutant to the MKS3 disorder of two other species; and our complete transgenic rescue from PKD, hydrocephalus, and abnormal cilia provide convincing evidence that the *bpck/bpck* mutant is a valuable model of PKD and MKS3. Although the mechanism of ciliary involvement in PKD is still not well understood, proteins of the primary cilium on renal tubular epithelial cells are clearly implicated. Our scanning electron micrographs and cilium measurements showing dysmorphic and elongated cilia in *bpck/bpck* mutants support this hypothesis; however, the cause-and-effect relationship of cilium length and cystogenesis requires further study to be understood. The *bpck/bpck* mutant adds another unique model to the growing repertoire of mouse models valuable for exploring the role of abnormal cilia in PKD. This first mouse model for MKS3 is appropriate for elucidating the cause of MKS3 and for testing preventive and therapeutic methods.

CONCISE METHODS

Mice

The *bpck* mutation arose spontaneously in 1979 in a mixed genetic background of a B6 and C3 substrain, B6C3-*tip*. We now maintain and analyze *bpck* on a "hybrid" background by alternately outcrossing +/*bpck* heterozygotes to B6C3FeF1/J *a/a* mice and intercrossing to identify +/*bpck* breeders for the next outcross generation (B6C3Fe *a/a -bpck*/J; JAX stock no. 8044, The Jackson Laboratory, Bar Harbor, ME). Because heterozygotes in both the colony and linkage cross are unaffected and 41 (20.5%) of 200 colony mice were mutants, *bpck* is inherited as a recessive allele. The Jackson Laboratory (JAX) adheres to the guidelines in the National Institutes of Health Guide for the Care and Use of Laboratory Animals. All procedures are approved by JAX Institutional Animal Care and Use Committee. All mice were maintained on a 14-h on/10-h off light cycle and fed NIH31 (6% fat) diet and acidified water *ad libitum*.

Linkage Analysis

We genetically mapped *bpck* using an intercross between +/*bpck* heterozygotes from the B6 incipient congenic stock and mice of the inbred *Mus musculus castaneus* strain CAST/EiJ and genome scanning for associations with single nucleotide polymorphisms and Massachusetts Institute of Technology markers.

Transgenic Rescue Crosses

Multiple transgenic lines were generated on the C57BL/6J background using BACs that contain two or more of the genes in the deleted region. No visible or histopathologic phenotypes have been observed in mice of any of the transgenic strains. Several of the cryopreserved strains are available from TJL (Table 4). +/*bpck* heterozygotes from the *bpck* stock were mated to mice hemizygous for BAC transgenes. Genotyped Tg/0 +/*bpck* progeny were backcrossed to +/*bpck* mice (partial backcross), and the progeny were genotyped for the transgene and *bpck* and observed for symptoms of PKD.

PCR, qPCR, Sequencing, and cDNA

Genomic DNA from tail tips was extracted with 97°C-heated 50 mM NaOH (pH 12.3) for 1 h and neutralized with 1 M Tris-HCl (pH 5.4). Standard PCR reactions used Master TaqKit (Eppendorf 0032002.650) with PCR conditions: One cycle at 97°C for 30 s, one cycle at 94°C for 15 s, 40 cycles of either 55 or 60°C for 30 s, one cycle at 72°C for 10 min, one cycle at 4°C for 15 min, and one hold cycle at 10°C. qPCR (quantitative PCR) was performed on a 7500 Real Time PCR System (http://www.appliedbiosystems.com). Sequencing PCR used Taqpolymerase from Roche Applied Science (1596594), and products were sequenced using a 50-cm array on an AB 3730xl with BigDye Terminator kit 3.1 (Applied Biosystems – Life Technologies, Carlsbad, CA). Postcycling cleanup of sequencing product used CleanSeq (Agencourt Bioscience Corporation, Beverly, MA). Results were analyzed with Sequencher v4.2 (Gene Codes Corp.). RNA was extracted

Table 4. BAC transgenic gene content and chromosomal insertion locations for BACs cryopreserved[a]

Transgene and BAC ID	Stock No.	Genes Included in BAC	Chromosomal Location
Tg(RP23-59K6)38Dn/J	7044	*Gem, Cdh17*	8A2
Tg(RP23-31I19)45Dn/J	6921	*Ppm2c, 1700123M08Rik,* ENSMUSG00000073995	10C2-D2
Tg(RP23-203A12)46Dn/J	8020	*Ppm2c, 1700123M08Rik, Tmem67,* ENSMUSG00000073995	5C1-3
Tg(RP23-203A12)48Dn/J	8022	*Ppm2c, 1700123M08Rik, Tmem67,* ENSMUSG00000073995	16C3-4
Tg(RP23-203A12)49Dn/J	8023	*Ppm2c, 1700123M08Rik, Tmem67,* ENSMUSG00000073995	9A2-5
Tg(RP24-229O13)50Dn/J	8024	*Ppm2c, 1700123M08Rik, Tmem67,* ENSMUSG00000073995	ND[b]
Tg(RP24-229O13)52Dn/J	8026	*Ppm2c, 1700123M08Rik, Tmem67,* ENSMUSG00000073995	2D-E1
Tg(RP24-229O13)53Dn/J	8027	*Ppm2c, 1700123M08Rik, Tmem67,* ENSMUSG00000073995	4C7
Tg(RP24-229O13)54Dn/J	8028	*Ppm2c, 1700123M08Rik, Tmem67,* ENSMUSG00000073995	10D1-3

[a]Note that *C430048L16Rik* was not intact in any of the transgenes.
[b]ND, not determined.

with TRIzol (Invitrogen 15596; Invitrogen – Life Technologies, Carlsbad, CA) and isolated DNA-free with RNAqueous-4PCR (Ambion 1914; Ambion – Life Technologies, Carlsbad, CA). cDNA was made with High Capacity Reverse Transcription Kit (Applied Biosystems 4368814). All PCR primers and TaqMan probes are displayed in Table 2.

Histology for Light Microscopy
Specimens for light microscopy were prepared by intracardiac perfusion with saline flush and Bouin fixative after animals were anesthetized with nonrecovery dosages of tribromoethanol (Avertin, prepared by JAX's Laboratory Animals Health Services, Bar Harbor, ME). Tissues were sectioned and stained by JAX's Histopathology & Microscopy Sciences. The confocal microscope was a Leica TCS NT (Depew, NY).

Image Analysis
The progression of cyst development, from postnatal day 9/10 to lethality, was followed with microcomputed tomography (microCAT II; Siemens Medical Solutions, Knoxville, TN) by JAX's *in vivo* Imaging Service. Mutant and normal-appearing controls from five litters were imaged at the same time every 3 to 4 d from 9 to 10 d of age to ESRD (19 to 21 d). Practical limitations of our imaging equipment prevented examination of younger mice.

Scanning Electron Microscopy
Kidneys for scanning electron microscopy were fixed in 2.5% glutaraldehyde in 0.1 M cacodylate buffer, dehydrated to 70% alcohol, freeze-fractured in liquid N_2, rehydrated in 0.1 M cacodylate buffer, treated with osmium, rinsed with buffer, dehydrated in graded alcohol up to 100% absolute, dried with hexamethyldisilazane, and coated with gold sputter to 19.32 g/cm³. Images were viewed on a Hitachi S3000 scanning electron microscopy microscope at 20 kV (Hitachi High Technologies America, Persippany, NJ). Cilia were measured

using Quartz PCI V.5.1 software (Quartz Imaging Corporation, Vancouver, Canada).

Immunohistochemical Studies
Kidney sections prepared as for light microscopy were stained with fluorescently tagged antibodies to megalin (sc-20609; Santa Cruz Biotechnology, Santa Cruz, CA; proximal tubules), aquaporin 2 1:300; collecting ducts and connecting tubules, Dr. E. Klussman, Leibniz-Institut für Molekulare Pharmakologie, Berlin, Germany), and calbindin-D28K (1:200; Sigma, St. Louis, MO; distal convoluted tubules and connecting tubules). Double labeling with antibodies to aquaporin 2 and calbindin distinguishes connecting tubules from collecting ducts and distal convoluted tubules.

Clinical Chemistries
Blood chemistries were determined by Affiliated Laboratories (Bangor, ME).

with scanning electron microscopy, the personnel of Clinical Pathology for urinalysis, and Weidong Zhang at Computational Sciences for data analysis. We thank Dr. James Mandell, President and Chief Executive Officer, Children's Hospital, Boston, for advice and reading the manuscript and Kenneth Johnson and Stephen Murray for critical review of the manuscript. Dr. Enno Klussman kindly provided the aquaporin 2 antibody.

DISCLOSURES

None.

REFERENCES

1. Grantham JJ, Nair V, Winklhofer F: Cystic disease of the kidney. In: *Brenner & Rector's The Kidney*, Vol. 2, 6th Ed., edited by Brenner BM, Philadelphia, WB Saunders Co., 2000, pp 1699–1730

2. Wilson PD: Polycystic kidney disease. *N Engl J Med* 350: 151–164, 2004

3. Guay-Woodford LM, Desmond RA: Autosomal recessive polycystic kidney disease: The clinical experience in North America. *Pediatrics* 111: 1072–1080, 2003

4. Torres VE, Harris PC: Mechanisms of disease: Autosomal dominant and recessive polycystic kidney disease. *Nat Clin Pract Nephrol* 2: 40–55, 2006

5. Esteban MA, Harten SK, Tran MG, Maxwell PH: Formation of primary cilia in the renal epithelium is regulated by the von Hippel-Lindau tumor suppressor protein. *J Am Soc Nephrol* 17: 1801–1806, 2006

6. Ansley SJ, Badano JL, Blacque OE, Hill J, Hoskins BE, Leitch CC, Kim JC, Ross AJ, Eichers ER, Teslovich TM, Mah AK, Johnsen RC, Cavender JC, Lewis RA, Leroux MR, Beales PL, Katsanis N: Basal body dysfunction is a likely cause of pleiotropic Bardet-Biedl syndrome. *Nature* 425: 628–633, 2003

7. Salonen R, Paavola P: Meckel syndrome. *J Med Genet* 35: 497–501, 1998

8. Guay-Woodford LM: Murine models of polycystic kidney disease: Molecular and therapeutic insights. *Am J Physiol Renal Physiol* 285: F1034–F1049, 2003

9. Bisgrove BW, Yost HJ: The roles of cilia in developmental disorders and disease. *Development* 133: 4131–4143, 2006

10. Smith UR, Consugar M, Tee LJ, McKee BM, Maina EN, Whelan S, Morgan NV, Goranson E, Gissen P, Lilliquist S, Aligianis IA, Ward CJ, Pasha S, Punyashthiti R, Malik Sharif S, Batman PA, Bennett CP, Woods CG, McKeown C, Bucourt M, Miller CA, Cox P, Algazali L, Trembath RC, Torres VE, Attie-Bitach T, Kelly DA, Maher ER, Gattone VH 2nd, Harris PC, Johnson CA: The transmembrane protein meckelin (MKS3) is mutated in Meckel-Gruber syndrome and wpk rat. *Nat Genet* 38: 191–196, 2006

11. Brown NE, Murcia NS: Delayed cystogenesis and increased ciliogenesis associated with the re-expression of polaris in Tg737 mutant mice. *Kidney Int* 63: 1220–1229, 2003

12. Davenport JR, Yoder BK: An incredible decade for the primary cilium: A look at a once-forgotten organelle. *Am J Physiol Renal Physiol* 289: F1159–F1169, 2006

13. Zhang Q, Taulman PD, Yoder BK: Cystic kidney diseases: All roads lead to the cilium. *Physiology* 19: 225–230, 2004

14. Wheatley DN, Wang AM, Strugnell GE: Expression of primary cilia in mammalian cells. *Cell Biol Int* 20: 73–81, 1996

15. Calvet JP: New insights into ciliary function: Kidney cysts and photoreceptors. *Proc Natl Acad Sci U S A* 100: 5583–5585, 2003

16. Singla V, Reiter JF: The primary cilium as the cell's antenna: Signaling at a sensory organelle. *Science* 313: 629–633, 2006

17. Nauli SM, Alenghat FJ, Luo Y, Williams E, Vassilev P, Li X, Elia AE, Lu W, Brown EM, Quinn SJ, Ingber DE, Zhou J: Polycystins 1 and 2 mediate mechanosensation in the primary cilium of kidney cells. *Nat Genet* 33: 129–137, 2003

18. Nauli SM, Rossetti S, Kolb RJ, Alenghat FJ, Consugar MB, Harris PC, Ingber DE, Loghman-Adham M, Zhou J: Loss of polycystin-1 in human cyst-lining epithelia leads to ciliary dysfunction. *J Am Soc Nephrol* 17: 1015–1025, 2006

19. Praetoroius HA, Spring KR: The renal cell primary cilium functions as a flow sensor. *Curr Opin Nephrol Hypertens* 12: 517–520, 2003

20. Bisceglia M, Galliani CA, Senger C, Stallone C, Sessa A: Renal cystic diseases: A review. *Adv Anat Pathol* 13: 26–56, 2006

21. Lu W, Peissel B, Babakhanlou H, Pavlova A, Geng L, Fan X, Larson C, Brent G, Zhou J: Perinatal lethality with kidney and pancreas defects in mice with a targeted Pkd1 mutation. *Nat Genet* 17: 179–181, 1997

22. Wu G, D'Agati V, Cai Y, Markowitz G, Park JH, Reynolds DM, Maeda Y, Le TC, Hou H Jr, Kucherlapati R, Edelmann W, Somlo S: Somatic inactivation of Pkd2 results in polycystic kidney disease. *Cell* 93: 177–188, 1998

23. Onuchic LF, Furu L, Nagasawa Y, Hou X, Eggermann T, Ren Z, Bergmann C, Senderek J, Esquivel E, Zeltner R, Rudnik-Schoneborn S, Mrug M, Sweeney W, Avner ED, Zerres K, Guay-Woodford LM, Somlo S, Germino GG: PKHD1, the polycystic kidney and hepatic disease 1 gene, encodes a novel large protein containing multiple immunoglobulin-like plexin-transcription-factor domains and parallel beta-helix 1 repeats. *Am J Hum Genet* 70: 1305–1317, 2002

24. Ward CJ, Hogan MC, Rossetti S, Walker D, Sneddon T, Wang X, Kubly V, Cunningham JM, Bacallao R, Ishibashi M, Milliner DS, Torres VE, Harris PC: The gene mutated in autosomal recessive polycystic kidney disease encodes a large, receptor-like protein. *Nat Genet* 30: 259–269, 2002

25. Bergmann C, Frank V, Kupper F, Schmidt C, Senderek J, Zerres K: Functional analysis of PKHD1 splicing in autosomal recessive polycystic kidney disease. *J Hum Genet* 51: 788–793, 2006

26. Pan J, Wang Q, Snell WJ: Cilium-generated signaling and cilia-related disorders. *Lab Invest* 85: 452–463, 2005

27. Marszalek JR, Ruiz-Lozano P, Roberts E, Chien KR, Goldstein LS: Situs inversus and embryonic ciliary morphogenesis defects in mouse mutants lacking the KIF3A subunit of kinesin-II. *Proc Natl Acad Sci U S A* 96: 5043–5048, 1999

28. Yoder BK, Tousson A, Millican L, Wu JH, Bugg CE Jr, Schafer JA, Balkovetz DF: Polaris, a protein disrupted in orpk mutant mice, is required for assembly of renal cilium. *Am J Physiol Renal Physiol* 282: F541–F552, 2002

29. Pazour GJ, Dickert BL, Vucica Y, Seeley ES, Rosenbaum JL, Witman GB, Cole DG: *Chlamydomonas* IFT88 and its mouse homologue, polycystic kidney disease gene tg737, are required for assembly of cilia and flagella. *J Cell Biol* 151: 709–718, 2000

30. Taulman PD, Haycraft CJ, Balkovetz DF, Yoder BK: Polaris, a protein involved in left-right axis patterning, localizes to basal bodies and cilia. *Mol Biol Cell* 12: 589–599, 2001

31. Yoder BK, Hou X, Guay-Woodford LM: The polycystic kidney disease proteins, polycystin-1, polycystin-2, polaris, and cystin, are co-localized in renal cilia. *J Am Soc Nephrol* 13: 2508–2516, 2002

32. Smith LA, Bukanov NO, Husson H, Russo RJ, Barry TC, Taylor AL, Beier DR, Ibraghimov-Beskrovnaya O: Development of polycystic kidney disease in juvenile cystic kidney mice: Insights into pathogenesis, ciliary abnormalities, and common features with human disease. *J Am Soc Nephrol* 17: 2821–2831, 2006

33. Mokrzan EM, Lewis JS, Mykytyn K: Differences in renal tubule primary cilia length in a mouse model of Bardet-Biedl syndrome. *Nephron Exp Nephrol* 106: e88–e96, 2007

34. Dawe HR, Smith UM, Cullinane AR, Gerrelli D, Cox P, Badano JL, Blair-Reid S, Sriram N, Katsanis N, Attie-Bitach T, Afford SC, Copp AJ, Kelly DA, Gull K, Johnson CA: The Meckel-Gruber syndrome proteins MKS1 and meckelin interact and are required for primary cilium formation. *Hum Mol Genet* 16: 173–186, 2007

35. Banizs B, Pike MM, Millican CL, Ferguson WB, Komlosi P, Sheetz J, Bell PD, Schwiebert EM, Yoder BK: Dysfunctional cilia lead to altered ependyma and choroid plexus function, and result in the formation of hydrocephalus. *Development* 132: 5329–5339, 2005

36. Ohnishi K, Melchers F, Shimizu T: Lymphocyte-expressed BILL-cadherin/cadherin-17 contributes to the development of B cells at two stages. *Eur J Immunol* 35: 957–963, 2005

37. Maj MC, MacKay N, Levandovskiy V, Addis J, Baumgartner ER, Baumgartner MR, Robinson BH, Cameron JM: Pyruvate dehydrogenase phosphatase deficiency: Identification of the first mutation in two brothers and restoration of activity by protein complementation. *J Clin Endocrinol Metab* 90: 4101–4107, 2005

38. McKee AE, Minet E, Stern C, Riahi S, Stiles CD, Silver PA: A genome-wide *in situ* hybridization map of RNA-binding proteins reveals anatomically restricted expression in the developing mouse brain. *BMC Dev Biol* 5: 14, 2005

39. Gattone VH 2nd, Tourkow BA, Trambaugh CM, Yu AC, Whelan S, Phillips CL, Harris PC, Peterson RG: Development of multiorgan pathology in the wpk rat model of polycystic kidney disease. *Anat Rec A Discov Mol Cell Evol Biol* 277: 384–395, 2004

40. Nauta J, Goedbloed MA, Herck HV, Hesselink DA, Visser P, Willemsen R, Dokkum RP, Wright CJ, Guay-Woodford LM: New rat model that phenotypically resembles autosomal recessive polycystic kidney disease. *J Am Soc Nephrol* 11: 2272–2284, 2000

41. Wang L, Weidenfeld R, Verghese E, Ricardo SD, Deane JA: Alterations in renal cilium length during transient complete ureteral obstruction in the mouse. *J Anat* 213: 79–85, 2008

42. Littell RC, Milliken GA, Stroup WW, Wolfinger RD: SAS System for Mixed Models, Cary, NC, SAS Institute, 1996